JPL NO. 9950 – 1098

N85-27465

CONDUCTING A WIND SENSING STUDY

Final Technical Report

for the period

December 31, 1983 to December 30, 1984

Contract No. JPL 956757

Principal Investigator

Robert L. Byer

G.L. No. 3821

Edward L. Ginzton Laboratory
W.W. Hansen Laboratories of Physics
Stanford University
Stanford, California 94305

This report was prepared for the Jet Propulsion Laboratory, California Institute of Technology, sponsored by the National Aeronautics and Space Administration.

March 1985

CONDUCTING A WIND SENSING STUDY

Robert L. Byer

Our study of global wind monitoring using Nd:YAG LIDAR has consisted of two efforts: 1. We completed a study of signal-to-noise requirements, and an analysis of how signal-to-noise determines wind velocity measurement accuracy. Based on this analysis of fundamentals, we found that a Nd:YAG-based system can be competitive with a CO_2-based system. Technological considerations, rather than atmospheric and signal-to-noise fundamentals, will be of greatest importance in determining the optimal system for a particular application. Our analysis was published in August 1984 in Applied Optics[1]. 2. We have developed hardware for a coherent Nd:YAG LIDAR system, and we are now integrating this hardware into a functioning system. The overall system design and performance will be described at the Coherent LIDAR conference this summer in England. The abstract and summary submitted to that conference describe the system[2].

Three laser components have been developed specifically for our coherent LIDAR system. A diode-pumped monolithic rod laser, to be used as a reference oscillator, was described in a February 1985 article in Optics Letters[3]. A high-power, single-mode ring laser, to be used as a master oscillator, was described in another article in the same issue[4]. The construction and performance of a high gain, multi-pass amplifier will be described at the 1985 CLEO meeting this May in Baltimore. Preliminary measurements and projected

performance of this amplifier are described in our abstract and summary submitted to that conference[5].

At this point we foresee no serious impediments to the completion and successful operation of our LIDAR system. We expect to be making atmospheric measurments this spring which will demonstrate the efficiency and stability of this system. We believe that these measurements will demonstrate the feasibility of Nd:YAG-based coherent LIDAR, both for wind velocity measurement and for sensing of hard targets.

REFERENCES

1. T. J. Kane, B. Zhou, and R. L. Byer, "Potential for coherent Doppler wind velocity lidar using neodymium lasers," in Applied Optics 23, p. 2477, (1984). Included as Appendix A.

2. T. J. Kane and R. L. Byer, "Coherent LIDAR Anemometry Using Nd:YAG Lasers: System Design and Performance," submitted to 3rd topical meeting on Coherent Laser Radar, Worcestershire, England, July 1985. Abstract and summary included as Appendix B.

3. B. Zhou, T. J. Kane, G. J. Dixon, and R. L. Byer, "Efficient, frequency-stable laser-diode-pumped Nd:YAG laser," in Optics Letters 10, p. 62, (1985). Included as Appendix C.

4. T. J. Kane and R. L. Byer, "Monolithic, unidirectional single-mode Nd:YAG ring laser," in Optics Letters 10, p. 65, (1985). Included as Appendix D.

5. T. J. Kane, W. J. Kozlovsky and R. L. Byer, "High-gain Multi-pass Amplification in a Single Nd:YAG Slab," to be presented at 1985 Conference on Lasers and Electro-Optics, Baltimore, May 1985. Abstract and summary included as Appendix E.

Reprinted from Applied Optics, Vol. 23, page 2477, August 1, 1984

Potential for coherent Doppler wind velocity lidar using neodymium lasers

Thomas J. Kane, Bingkun Zhou, and Robert L. Byer

Existing techniques for the frequency stabilization of Nd:YAG lasers operating at 1.06 μm, and the high-gain amplification of radiation at that wavelength, make possible the construction of a coherent Doppler wind velocity lidar using Nd:YAG. Velocity accuracy and range resolution are better at 1.06 μm than at 10.6 μm at the same level of the SNR. Backscatter from the atmosphere at 1.06 μm is greater than that at 10.6 μm by ~2 orders of magnitude, but the quantum-limited noise is higher by 100 also. Near-field attenuation and turbulent effects are more severe at 1.06 μm. In some configurations and environments, the 1.06-μm wavelength may be the better choice, and there may be technological advantages favoring the use of solid-state lasers in satellite systems.

I. Introduction

It is possible to measure a velocity component of the wind by measuring the Doppler shift of electromagnetic radiation scattered by particles entrained in the wind. Microwave radar systems at a wavelength of 10 cm provide data on the structure and development of storms using raindrops as the scattering particles.[1] Microwave radar systems can also detect and interpret signals arising from reflections taking place due to density fluctuations in clear air.[2] Laser radar systems operating at the 10.6-μm carbon dioxide laser line have successfully measured the wind velocity by detecting the radiation scattered from dust particles (aerosols), which are found even in the clearest atmospheric air.[3] The technology of wind velocity measurement using CO_2 lasers has developed to the point where a mobile system has been built to study the adequacy of the return signal in different geographical regions. The possibility of installing such a system on a satellite or space shuttle is being seriously considered.[4]

These microwave and far-IR systems are described as coherent systems because their operation requires a comparison of the phase of the scattered signal with the phase of a reference signal at the detector. This reference signal must have good frequency stability (or coherence) if the system is to be accurate. Coherent microwave and far-IR systems generally transmit short pulses and achieve range resolution by measuring the time delay of the return signal. Only the component of wind velocity parallel to the beam is measured in this type of system.

In this paper we examine the potential for remote wind sensing lidar systems based on neodymium lasers. We show that at a given level of the SNR, the 1.06-μm wavelength of Nd:YAG offers smaller velocity error and better range resolution than is possible using the 10.6-μm wavelength of CO_2 lasers. Currently available data indicate that at similar levels of transmitted power, the SNR at 1.06 μm for typical atmospheric conditions is the same as the SNR at 10.6 μm, if the effects of atmospheric turbulence are not considered. Atmospheric turbulence is a greater problem at 1 μm than at 10 μm, but for some system configurations it is not an important problem for either wavelength.

Neodymium solid-state systems may offer technological advantages compared with CO_2 laser-based systems. The rapid progress in high-power diode semiconductor lasers may lead to diode-pumped Nd:YAG systems, which are more efficient than CO_2 lasers and offer longer operating lifetimes for satellite-based measurements. Finally, we briefly describe the Nd:YAG-based remote wind sensing lidar under construction at Stanford University.

II. Velocity Estimate Error

The pulse pair algorithm is a well-understood way to extract an estimate of average frequency (and thus velocity) from a random signal with a Gaussian-shaped spectrum.[5] For a particular SNR the expected rms velocity error is given by

$$\delta v = \frac{\lambda}{4\pi}\left(\frac{f}{2NL}\right)^{1/2}\left(2\pi^{1/2}W + \frac{16\pi^2W^2}{\mathrm{SNR}} + \frac{1}{\mathrm{SNR}^2}\right)^{1/2}. \quad (1)$$

The authors are with Stanford University, Edward L. Ginzton Laboratory, Stanford, California 94305.

Received 22 October 1983.
0003-6935/84/152477-05$02.00/0.

where f is the sampling frequency, N is the number of pulses averaged, t is the duration of a transmitted pulse, L is the ratio of the length of a range gate to the length of a pulse, and λ is the wavelength.[6] The value W is a measure of the frequency spread of the return signal in the absence of any noise and is given by

$$W = \frac{1}{v_{Ny}}(v_{bw}^2 + v_{atm}^2)^{1/2}, \tag{2}$$

where v_{Nv} is the maximum unaliased velocity as determined by the Nyquist criterion, $v_{Ny} = f\lambda/2$, v_{bw} is the velocity uncertainty corresponding to the bandwidth of the transmitted pulse, and v_{atm} is the standard deviation of the velocity distribution in the measured volume due to turbulence and wind shear. Note that for a fixed value of v_{Nv} the shorter wavelength will require a proportionally faster sampling frequency f. For a Fourier transform-limited Gaussian pulse, the spread due to bandwidth is given by $v_{bw} = \lambda/4\pi t$.

The effect of wavelength on velocity error depends on the other parameters involved. We present a few examples. If the SNR is fixed, the 1-μm system always gives a smaller velocity uncertainty. However, the size of the advantage varies from case to case. The 1-μm wavelength is also able to provide greater spatial resolution. We examine velocity error and spatial resolution for four cases: that of error dominated by wind variability v_{atm}, by pulse length v_{bw}, by noise with low SNR, and by noise with moderate SNR.

A. High SNR: Wind Variability Dominates Error

In the regime where the predominant source of error is the range of velocities in the measured volume and the average velocity is desired, the expected error in the average velocity simplifies to

$$\delta_v = (2\pi^{3/2}v_{atm}\lambda/NLt)^{1/2}/4\pi. \tag{3}$$

With all other factors held constant, the velocity error at 1 μm is less than that at 10 μm by a factor of the square root of 10. This improvement is due to the observation of more full cycles of the return signal from a particular range gate at 1 μm than at 10 μm because of the greater Doppler shift. The mean square fractional frequency error decreases with the number of cycles counted. A useful figure of merit is the product of the velocity variance δv^2 and the range resolution given by $\delta R = cLt/2$, where c is the speed of light. Ignoring constant factors, this yields

$$\delta v^2 \delta R \propto v_{atm}\lambda/N. \tag{4}$$

A ten times better range resolution is possible at 1 μm than at 10 μm, with velocity error held constant.

B. High SNR: Transmitted Pulse Bandwidth Dominates Error

If the SNR is high and high-range resolution is desired, the frequency uncertainty due to the limited pulse duration becomes the predominant error source. This case yields the same uncertainty relations that apply to nonstochastic hard targets. The equation for the velocity uncertainty becomes

$$\delta v = \lambda(\pi^{1/2}/2NL)^{1/2}/4\pi t. \tag{5}$$

The velocity resolution at 1 μm is 10 times better than at 10 μm for this case. The product of range resolution and velocity resolution becomes, ignoring constant factors,

$$\delta v \delta R \propto \lambda(L/N)^{1/2}. \tag{6}$$

The advantage of a shorter wavelength is greater in the case of nonrandom targets. In this case it is not the mean square error but the rms error that increases linearly with wavelength.

C. Low SNR

When the SNR is very low (of the order of 1) it is the last term of Eq. (1) that dominates. In this case the velocity uncertainty becomes

$$\delta v = \lambda(f/2NLt)^{1/2}/4\pi\mathrm{SNR}. \tag{7}$$

Since the sampling frequency f must be greater at shorter wavelengths for the same maximum velocity, as determined by the Nyquist criterion, this equation is more useful for comparison if written in terms of the maximum velocity $v_{Ny} = f\lambda/2$. Equation (7) then becomes

$$\delta v = (\lambda v_{Nv}/NLt)^{1/2}/4\pi\mathrm{SNR}. \tag{8}$$

Once again the velocity resolution is better at 1 μm than at 10 μm by a factor of the square root of 10. A lower SNR at 1 μm can yield the same velocity error. The range resolution–velocity resolution trade-off, again dropping constants, is

$$\delta v^2 \delta R = \frac{\lambda v_{Nv}}{N \cdot \mathrm{SNR}^2} \tag{9}$$

D. Intermediate Case: Moderate SNR

In the case of moderate SNR, Eq. (1) cannot be written simply. All terms contribute to the velocity error. However, a few comments can be made.

The velocity error advantage at 1 μm is between 10 and the square root of 10. The advantage in range resolution, other things held constant, is in all cases a factor of 10.

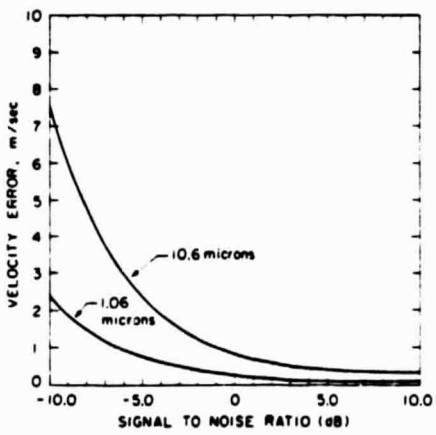

Fig. 1. Expected velocity error plotted as a function of SNR. Both pulse length and range gate are 3 μsec. Maximum unaliased velocity v_{Nv} is 25 m/sec, and rms wind variability v_{atm} is 0.3 m/sec. Error at 10.6 μm is slightly more than $\sqrt{10}$ times as high as error at 1.06 μm.

If a particular maximum velocity error is acceptable, a measurement at 1 μm can be made at a lower SNR than is possible at 10 μm. At low SNR the 1-μm SNR can be lower by $\sqrt{10}$. At higher SNR, the velocity resolution degrades more slowly as the SNR goes down, and the allowable SNR reduction possible at 1 μm is in all cases $> \sqrt{10}$.

Figure 1 is a plot of an expected single-pulse velocity error calculated using Eq. (1). The pulse length and range gate are both 3 μsec. The value of v_{Ny} is 25 m/sec, and the rms wind variability v_{atm} is 0.3 m/sec. For this case the ratio of the errors is $\sim\sqrt{10}$ at all values of SNR. For shorter pulse length or less wind variability the advantage of 1.06 μm compared with 10.6 μm is larger.

III. Signal-to-Noise Considerations

A. Atmospheric Beta

The backscatter cross section of a sphere of known radius and index of refraction can be calculated exactly. In the Rayleigh scattering limit, when the size of the wavelength is large compared with the size of the scattering sphere, the backscatter cross section is proportional to the inverse fourth power of the wavelength. If all aerosol particles were small compared with 1 μm, the value of β, the backscatter cross section per unit volume of air, would be 10,000× higher at 1 μm than at a wavelength of 10 μm.

In fact the particles containing the greatest fraction of the aerosol mass are near 1 μm in radius, and the advantage at 1 μm is considerably less than 10,000. Kent estimates that the typical ratio of backscatter at 1 μm to backscatter at 10 μm is in the 40–200 range for air in the free troposphere.[7] The backscatter at 10 μm is a very sensitive function of the number of fairly large particles (>1 μm),[8] and thus it is the more variable of the two values. For tropospheric air over the oceans, and in the stratosphere during times of volcanic inactivity, the advantage at 1 μm will be as high as 200. This is significant because these are the conditions that would result in very low return signals at 10 μm.

The statistical distribution of β values, for different altitudes and regions, is not known well. As data from the SAGE and SAM II satellite sensors become available,[9] much more will be known about atmospheric attenuation (and thus backscatter) at 1 μm. It is approximately true that in the troposphere the backscatter from aerosols at 1 μm is the same as the backscatter from the air itself (molecular backscatter).[10] This value is 3×10^{-8} m^{-1} for air at 0°C and 1-atm pressure. Very clean air would have a backscatter value due to aerosols of 10^{-9} m^{-1}.

B. Coherence of Return Signal

For minimum background interference, the detected signal must be collected from a single diffraction-limited spot on the focal plane of the telescope. If the source of the collected light were a fixed point at infinity, such as a star, the amount of light collected in a single diffraction-limited spot would be severely limited by the optical distortion caused by the turbulent atmosphere. In the visible, during times of moderate turbulence, it becomes impossible to increase the power collected in a single spatial mode once the diameter of the telescope exceeds a few centimeters. This would also be the case for a bistatic laser radar system. Clifford and Lading[11] have shown that for a system where the same optics are used for both transmission and collection of the signal (a monostatic system), moderate turbulence is less of a disadvantage. Without turbulence, a system collecting light in a single spatial mode receives a signal strongly peaked at the focus of the telescope and attenuated at both shorter and longer ranges. This effect leads to received powers a few orders of magnitude greater at the focus than at close range. The effect of moderate turbulence is to reduce the signal from the focal volume but to increase the signal from closer range.

Turbulence is a potentially important parameter at $\lambda = 1.06$ μm, especially for ground-based systems. The transverse atmospheric coherence length ρ_0 has a $\lambda^{6/5}$ dependence. Thus ρ_0 at 10.6 μm is 15.8× larger than at 1.06 μm. A reasonable approximation for SNR reduction due to turbulence in the focused beam case is

$$F_0 = 1/(1 + D^2/4\rho_0^2), \tag{10}$$

where D is the optics diameter and F_0 is the SNR reduction factor relative to the zero turbulence case.[12] Consider the case where ρ_0 computed for 10.6 μm is equal to the telescope diameter D. The value of F_0 is 0.8. Using the scaling law for ρ_0 mentioned above, the value of F_0 at 1.06 μm is 0.015.

The problem of near-field attenuation of the signal received by diffraction-limited systems is also greater since the area of a diffraction-limited spot for 1-μm radiation is 1/100 the area of a diffraction-limited spot for 10-μm radiation. It may be desirable to detect more than a single spatial mode of the return signal at 1 μm.

In some configurations the effects of turbulence and near-field attenuation are greatly reduced. One example is a system with a small aperture telescope. Another is the case of a telescope above the atmosphere. It is turbulence immediately in front of the telescope that is responsible for most of the reduction in signal. Turbulence in the scattering volume has no effect, since the scattering process is incoherent. Near-field attenuation is not a problem for a satellite-based system, since the signal from the near field is not of interest.

C. Noise

Quantum-limited noise levels have been achieved for coherent detection of 10-μm radiation. At 1 μm, reaching this limit is much easier due to the lower detector dark current and greater amount of quantum noise. The quantum noise is given by

$$N = Bh\nu, \tag{11}$$

where B is the detection system bandwidth, and $h\nu$ is the energy of a single photon at the wavelength of interest. At 1 μm the photon energy is 10× greater and the bandwidth 10× larger for the same range of veloci-

ties. Thus the noise is 100× greater at 1 μm than at 10 μm for quantum-limited detection.

As stated above, the atmospheric β and thus the signal at 1.06 μm are ~40–200× that at 10.6 μm. The quantum-limited noise at the shorter wavelength is 100× as great as that at the CO_2 wavelength. The result is that the SNR at 1.06 μm will typically be about the same as that at 10.6 μm. In very clear air, the SNR at 1 μm will exceed that at 10 μm.

IV. Energy Requirements—Ideal Case

The transmitted energy needed to receive a signal equal to the noise can be calculated if losses due to turbulence and collection inefficiency are neglected. The basic equation for the SNR is

$$\mathrm{SNR} = \eta\lambda\beta E\pi d^2/8R^2Bh. \tag{12}$$

where η = detection efficiency,
E = pulse energy,
d = telescope diameter,
R = range of return signal with telescope focused there,
B = system bandwidth, and
h = Planck's constant.

First, we calculate the minimum value of β for the moderate-sized ground-based system under construction at Stanford. We assume optimal conditions with no loss due to turbulence. We also assume 100% collection and detection efficiency, quantum-limited detection, a transmitted pulse energy of 100 mJ, a range of 10 km, telescope diameter of 40.6 cm (16 in.), and a system bandwidth and digitization rate of 100 MHz. The value of β at which signal equals noise is 10^{-9} m^{-1}. This is on the extreme low end of the range of backscatter values found in the troposphere at 1 μm. Of course, actual system performance will not be this high, as collection inefficiencies and turbulent effects will lessen the signal. If the pulse length is 3 μsec, and the range gate is the same as the pulse length, the single-pulse velocity error is 0.33 m/sec for a 0.9-km depth resolution at a range of 10 km, when all error is due to noise.

A second example of interest is a satellite-based system with a 1-m diam receiving telescope at an 800-km altitude above the earth's surface. For a β value of 3×10^{-7} m^{-1} (molecular scatter = aerosol scatter) we find that the required pulse energy for SNR = 1 is 3 J.

V. Neodymium-based Coherent lidar

Pulsed reference-beam coherent lidar systems put two principal requirements on the laser technology: first, the low-power oscillator must be stabilized so that the frequency drift during the pulse round trip time contributes only a small fraction of the allowable frequency error; second, a high-energy pulse must be transmitted at a known offset frequency from the oscillator to well within the allowable frequency error. A system operating at 1 μm with a velocity error of 0.5 m/sec must have a frequency stability well under 1 MHz. For a range of 15 km, the required duration of this stability is 100 μsec.

The necessary frequency stability has been demonstrated in Nd:YAG at low powers.[13,14] Frequency shifting the 1-μm wavelength is easily done by acoustooptic or electrooptic modulation. The Nd:YAG laser offers the additional advantage of extremely high-gain amplification due to the high-energy storage density possible in solid-state lasers. Systems with gains as high as 54 dB have been built.[15] The master oscillator power amplifier (MOPA) configuration for a laser transmitter is ideally suited for the intrinsically high-gain Nd:YAG laser. Frequency chirp during amplification is extremely low.

A system operating from a satellite will see a large Doppler shift due to the motion of the satellite. For example, at a 7.7-km/sec ground velocity with an angle of observation 10° from vertical, the frequency offset is 2.5 GHz. Nd:YAG can be easily tuned over a 30-GHz wide range. We have demonstrated a small Nd:YAG oscillator pumped by a semiconductor diode laser with a tuning range of 16 GHz. The entire oscillator and its pump laser weigh a fraction of a kilogram.

Radiation at 1.06 μm can be amplified to large energies at high repetition rates. Pulse energies of 1 J are available from Nd:YAG systems at repetition rates of 25 Hz with rod geometry lasers. Repetition rates up to 100 Hz appear feasible with zigzag slab geometry lasers.[15] Higher pulse energies at repetition rates up to a few hertz are available using Nd:glass amplifiers in the slab configuration. A pulse energy of 5 J at 2-μm duration and a repetition rate of 1 Hz have been produced by a combination Nd:YAG–Nd:glass system for use in combustion research.[15]

The operating efficiency of conventional Nd lasers is lower than the efficiency of CO_2 lasers. Pulsed YAG lasers operate at ~1% electrical-to-optical efficiency, while CO_2 lasers operate at ~5% efficiency. The inefficiency of neodymium systems is due to the low absorption of the flashlamp light by the Nd ions. Lasers optically pumped by narrowband light can be extremely efficient. Semiconductor diode lasers made from gallium aluminum arsenide emit at the wavelength of 0.81 μm, which is efficiently absorbed by the Nd ion. The overall efficiency of diode-pumped Nd:YAG is near 10%. Large arrays of diode lasers will be needed for pulsed pumping, and it is not yet clear that energies >1 J will be possible. Although diode arrays will certainly be costly, the very low voltage requirement (2 V), high efficiency, and inherent reliability of an all-solid-state design would be ideal for satellite use.

VI. Stanford Nd:YAG Remote Wind Sending lidar

We have initiated construction of a coherent lidar system using Nd:YAG. Although current technology is adequate, we are trying to increase the efficiency, compactness, and simplicity of the system by developing a single-crystal diode-pumped oscillator and a very high-gain multipass amplifier. Other components of the system will be conventional.

Figure 2 is a schematic of the system. A diode laser pumps a Nd:YAG crystal oscillator to which coatings are applied directly. The crystal is conduction cooled.

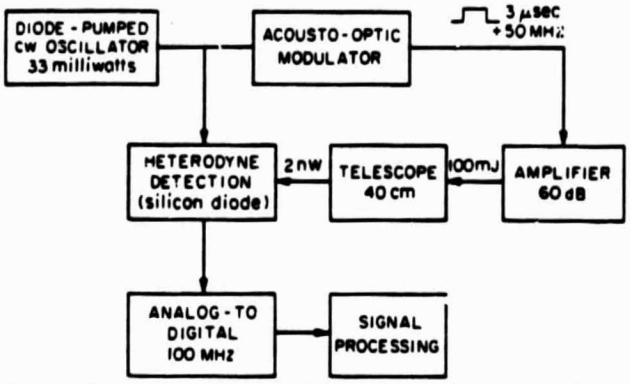

Fig. 2. Schematic of coherent lidar system under construction at Stanford. The diode-pumped single-crystal laser oscillator achieves excellent frequency stability (200 kHz in 0.1 sec) without active stabilization. The amplifier makes use of a single slab which is multipassed to achieve high gain efficiently. Other components are conventional.

In conventional laser oscillators, water cooling and mirror motion are major sources of frequency instability. We expect very good frequency stability without the necessity of feedback stabilization in this miniature diode-pumped crystal oscillator. Preliminary measurements of the beat frequency width between two independent oscillators yielded 200 kHz over a 0.1-sec integration time.

Most of the oscillator output is directed to the multipass amplifier. A zigzag slab of Nd:YAG[16] is used as the amplifier. The slab offers very low thermal distortion, high gain per pass due to the longer zigzag path, and the ability to pass several beams through the same volume of Nd:YAG and easily separate the beams outside the crystal.

An acoustooptic modulator is used to chop the amplified beam into pulses of a few microseconds duration. The modulator also creates a 50-MHz frequency offset to provide for Doppler detection at the intermediate frequency. Following pulse shaping by the acoustooptic modulator, the pulses are further amplified by a final saturated Nd:YAG amplifier.

The pulses are transmitted by a 40-cm diam telescope. The return signal is to be collected by the same telescope, mixed with a small fraction of the power from the local oscillator, and detected by a silicon photodiode. The signal is digitized at a rate of 100 MHz and analyzed conventionally.

We expect usable signal return (SNR > 1) at ranges up to 10 km, for a vertical beam path.

VII. Conclusion

A Nd:YAG-based coherent Doppler remote wind sensing system could be built using existing technology. A 1-μm system results in a smaller expected velocity error than a 10-μm system at the same level of SNR. The reduction in error is by a factor of between $\sqrt{10}$ and 10. The range resolution improves by a factor of 10 if the velocity error is held constant. A system operating at 1 μm can operate at a SNR at least 3× smaller than that of a 10-μm system and achieve the same velocity resolution.

The return signal from the atmosphere at the 1.06-μm wavelength of Nd:YAG will be 40–200× stronger than the return at the 10.6-μm CO_2 wavelength. The quantum-limited noise will be 100× higher at the Nd wavelength than at the CO_2 wavelength. Thus the SNR will be about the same.

The problems of signal reduction due to turbulence and near-field attenuation are greater at 1 μm. Systems with a small aperture and systems looking down from above the atmosphere will be troubled by these problems to only a small extent. Our large-aperture single-detector ground-based system will suffer signal reduction under turbulent conditions. We plan to study the severity of this effect.

The technologies of both carbon dioxide lasers and Nd lasers are well developed. Carbon dioxide lasers are more efficient than conventional flashlamp-pumped Nd lasers. Neodymium lasers are physically smaller. The developing technology of laser-diode-pumped Nd:YAG may improve Nd:YAG efficiency to the same level as CO_2 lasers. Although such lasers will be expensive, they may prove advantageous for satellite-based coherent lidar systems.

This work was supported by NASA under contract NAG-182. Bingkun Zhou is a visiting scholar from Tsinghua University, Radio Science Department, Beijing, China.

This paper is based on one presented at the Second Topical Meeting on Coherent Laser Radar, Aspen, Colo., 1–4 Aug. 1983.

References

1. P. S. Ray, R. J. Doviak, G. B. Walker, D. Sirmans, J. Carter, and B. Bumgarner, J. Appl. Meteorol. 14, 1521 (1975).
2. R. J. Doviak and C. T. Jobson, J. Geophys. Res. 84, 697 (1979).
3. M. J. Post, R. A. Richter, R. M. Hardesty, T. R. Lawrence, and F. F. Hall, Proc. Soc. Photo-Opt. Instrum. Eng. 300, 60 (1981).
4. R. M. Huffaker, Ed., "Feasibility Study of Satellite-Borne Lidar Global Wind Monitoring System," NOAA Tech. Mem. ERL WPL-37 (1978).
5. D. S. Zrnic, IEEE Trans. Geosci. Electron. GE-17, 113 (1979).
6. R. V. Hess, P. Brockman, C. H. Bair, L. D. Staton, C. D. Lytle, L. M. Laughman, and M. L. Kaplan, Proc. Soc. Photo-Opt. Instrum. Eng. 415, 52 (1983).
7. G. S. Kent, Institute for Atmospheric Optics & Remote Sensing, Hampton, Va.; personal communication.
8. G. S. Kent, G. K. Yue, U. O. Farrukh, and A. Deepak, Appl. Opt. 22, 1655 (1983).
9. M. P. McCormick, P. Hamill, T. J. Pepin, W. P. Chu, T. J. Swissler, and L. R. McMaster, Bull. Am. Meteorol. Soc. 60, 1038 (1979).
10. P. B. Russell, B. M. Morley, J. M. Livingston, G. W. Grams, and E. M. Patterson, Appl. Opt. 21, 1541 (1982).
11. S. F. Clifford and L. Lading, Appl. Opt. 22, 1696 (1983).
12. S. F. Clifford and S. M. Wandzura, Appl. Opt. 20, 514 (1981).
13. H. G. Danielmeyer, "Progress in Nd:YAG lasers," in *Lasers*, Vol. 1, A. K. Levine and A. J. DeMaria, Eds. (Marcel Dekker, New York, 1976).
14. Y. L. Sun and R. L. Byer, Opt. Lett. 7, 408 (1982).
15. P. J. Brannon, F. R. Franklin, and E. D. Jones, Appl. Opt. 21, 1758 (1982).
16. T. J. Kane, R. C. Eckardt, and R. L. Byer, IEEE J. Quantum Electron. QE-19, 1351 (1983).

FEBRUARY 1985

VOLUME 10 NUMBER 2

Optics Letters

A publication of the

OPTICAL SOCIETY OF AMERICA

Efficient, frequency-stable laser-diode-pumped Nd:YAG laser

Bingkun Zhou,* Thomas J. Kane, George J. Dixon, and Robert L. Byer

Ginzton Laboratory, Stanford University, Stanford, California 94305

Received October 1, 1984; accepted November 21, 1984

We have designed and tested a laser-diode-pumped monolithic Nd:YAG oscillator. The electrical-to-optical slope efficiency was 6.5%. The frequency jitter was less than 10 kHz over a 0.3-sec period, the best frequency stability reported for a Nd:YAG laser to date.

End pumping of a miniature Nd:YAG laser with a gallium–aluminum–arsenide (GaAlAs) laser diode is an attractive means of obtaining a long-lived, efficient cw Nd:YAG laser. For many applications a miniature Nd:YAG laser provides capabilities that the laser diode itself cannot. The spatial and temporal coherence of the Nd:YAG oscillator exceeds that of the laser-diode pump. In addition, the Nd:YAG oscillator output can be amplified by high-gain Nd:YAG amplifiers.

Our goal for laser-diode pumping was to demonstrate a low-power, efficient Nd:YAG laser oscillator for applications in remote coherent Doppler anemometry.[1] Previous work has shown that conventional flashlamp-pumped, water-cooled Nd:YAG oscillators are limited to a frequency stability of 0.2 MHz over 5 msec by flashlamp- and coolant-induced instabilities.[2] This work shows that laser-diode-pumped Nd:YAG oscillators can be operated at a frequency stability that far exceeds conventionally pumped stabilized Nd:YAG oscillators.

Recently, the efficiency and the output power of GaAlAs laser diodes have improved dramatically. Laser diodes with cw single-mode outputs of 20 mW are commercially available,[3] and, with some loss of mode quality, cw laser diodes of 40 and 100 mW are available.[4] We have used these laser diodes to pump monolithic Nd:YAG rod lasers and have achieved an electrical-to-optical slope efficiency of 6.5%. The observed Nd:YAG oscillation threshold was at 2.3 mW of laser-diode output power, which is a small fraction of the rated output power. Thus the goal of efficient operation at a conservative level of diode power was achieved. The highest Nd:YAG cw output power reached was 4.4 mW at an overall electrical-to-optical efficiency of 1.5%.

The laser-diode-pumped Nd:YAG laser oscillates in a single axial and transverse mode. The laser resonator consists of the Nd:YAG rod itself, which is rigid and thus resistant to acoustic noise. Cooling takes place by conduction and thus is stable. The laser-diode pump source is extremely stable if the diode current and the temperature are stable. Thus extreme frequency stability and long coherence length are possible. We observe a frequency jitter of less than 10 kHz (1 part in 3×10^{10}) in 0.3 sec.

The narrow but strong absorption lines of Nd:YAG make it well suited for narrow-band optical pumping. When the pump beam is collinear with the resonator (end pumping), the overlap between the pumped volume and the Nd:YAG TEM_{00} mode can be good and the absorption and coupling efficiency high. A number of workers have built neodymium lasers end pumped with diodes. Light-emitting diodes have been used to end pump Nd:YAG fibers.[5] Superluminescent diodes have end pumped Nd:YAG rods.[6] Laser diodes have been used to end pump the stoichiometric neodymium compound $LiNdP_4O_{12}$ with a 1.5% electrical-to-optical slope efficiency.[6] This Letter reports the highest efficiency for Nd:YAG to date and contains the first reported measurements of frequency stability.

We fabricated Nd:YAG rods of length 5 mm and diameter 2 mm. Each end had a radius of curvature of 19 mm. One end was coated to be high-reflecting at 1064 nm and high-transmitting at the pump wavelength of 809 nm. The other end had a transmission of 0.3% at 1064 nm and was reflecting at 809 nm. Figure 1 shows a schematic of the end-pumped Nd:YAG oscillator. The output of a constricted double-heterojunction large-optical-cavity (CDH-LOC)[8] diode laser was collected and focused by a gradient-index lens (Selfoc lens[9]) of 0.25 pitch. A magnification of 20× matched the diode pump beam to the TEM_{00} mode of the monolithic resonator. The TEM_{00} mode waist of the Nd:YAG resonator had a radius $w_0 = 39.4\ \mu m$, and the calculated radii for the two axes of the elliptical pump beam were $w = 10.4$ and $w = 37.2\ \mu m$. The pump laser was selected to operate at 806 nm at room temperature. Efficiency data reported here were obtained when the diode temperature was in the range 20–25°C.

Alignment of these small lasers is not difficult. The fabrication tolerance for parallelism between the two mirror faces is detemined by the ratio of useful aperture to mirror curvature and in our case was an easily ob-

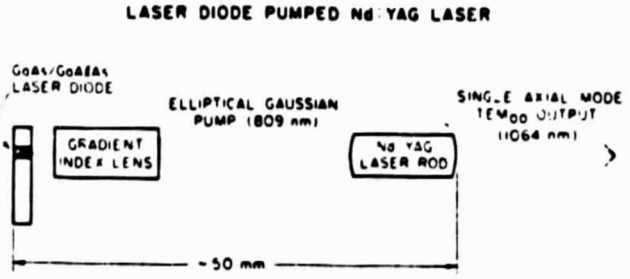

Fig. 1. Schematic of the laser diode, gradient-index lens, and monolithic Nd:YAG oscillator.

0146-9592/85/020062-03$2.00/0

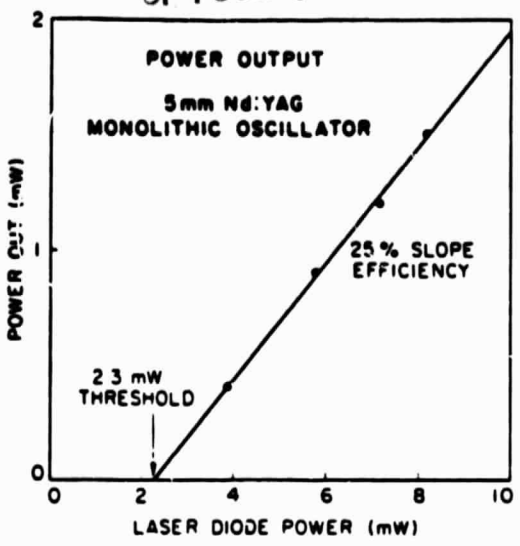

Fig. 2. Power input versus output for the 5-mm Nd:YAG rod end pumped with the CDH-LOC laser, focused by a quarter-pitch Selfoc lens.

tained ±3°. Alignment of the pump to the resonator was most easily achieved by looking through the output face of the Nd:YAG to see the fluorescence at 1.06 μm. The pump is reflected at the faces and thus passes through the rod more than once. When all passes overlap, the laser is aligned. The lowest threshold alignment always corresponded to the optimum alignment for TEM_{00} operation. With the CDH-LOC index-guided diode laser, TEM_{00} operation was possible at all pump powers. The threshold of the second axial mode occurred at a Nd:YAG output power of 1.2 mW.

Figure 2 is a plot of output power at 1064 nm as a function of pumping power at 806 nm. Slope efficiency was 25%, and the threshold pump power was 2.3 mW. The electrical-to-optical slope efficiency of the diode was 26%, so the overall electrical-to-optical slope efficiency was 6.5%. Overall efficiency, as opposed to slope efficiency, was low, because the laser diode had been damaged in earlier experiments and had a high threshold.

Similar measurements were made with a Nd:YAG rod of 3-mm length. The slope efficiency was reduced to 17% for the diode-pumped case. With dye-laser pumping at the very strongly absorbed wavelength of 590 nm, efficiency did not depend on rod length. Thus we believe that the 3-mm rod was too short for optimum diode-pumped efficiency. For the 3-mm rod, the threshold of the second axial mode could be reached only with dye-laser pumping and was found to occur at 8 mW of output power.

We tested other laser-diode pump sources and found that the beam quality of the laser-diode pump was important. The gain-guided single-stripe laser produced by Spectra Diode Laboratories had an astigmatic beam. Thus the spot size after a single spherical lens was larger than that of the index-guided CDH-LOC laser. Absorption was lower, because the gain-guided laser oscillated in several axial modes and thus had a linewidth large compared with the width of the Nd:YAG absorption lines. TEM_{00} operation was more difficult to achieve, and slope efficiency was reduced to 12%. The 40-mW power available from this laser diode, however, resulted in a 4.4-mW output at 1064 nm. The overall electrical-to-optical efficiency was 1.5%.

The polarization of the monolithic lasers was indeterminate unless a small stress was applied transversely to the rod. The 1064-nm polarization was always parallel and never perpendicular to the applied stress.

The laser-diode pump wavelength must be selected to match the absorption of Nd:YAG. Figure 3 is a plot of Nd:YAG optical absorption as a function of wavelength. The dashed horizontal line is at a level corresponding to 50% absorption in 4 mm. The data points in Fig. 3 show the absorption measured by scanning the CDH-LOC diode temperature. Diode temperature control is a convenient way to match the laser-diode output wavelength to the absorption of Nd:YAG and thus to ease the tolerance on diode wavelength. The average temperature-tuning coefficient for the laser diode of Fig. 3 is 0.35 nm/°C.

A primary goal of this work was to measure the frequency stability of monolithic, laser-diode-pumped Nd:YAG lasers. We pumped two Nd:YAG oscillators with the same laser diode and mixed the output of the two oscillators on the face of a photodiode. The beat signal was observed with a spectrum analyzer. A plastic case was used to isolate the two lasers from fast temperature fluctuations. Other than that, no effort was made to stabilize the lasers. A heater was attached to one laser to permit some tunability. The temperature-tuning coefficient for any monolithic Nd:YAG laser operating at 1064 nm is 3.1 GHz/°C. The axial mode spacing of the 5-mm rods is 16.5 GHz, so a temperature range of only a few degrees was needed to ensure that the beat signal was within the 1-GHz bandwidth of the detector.

We observed the beat signal for several hours and noted a typical rate of frequency drift of 300 kHz/min.

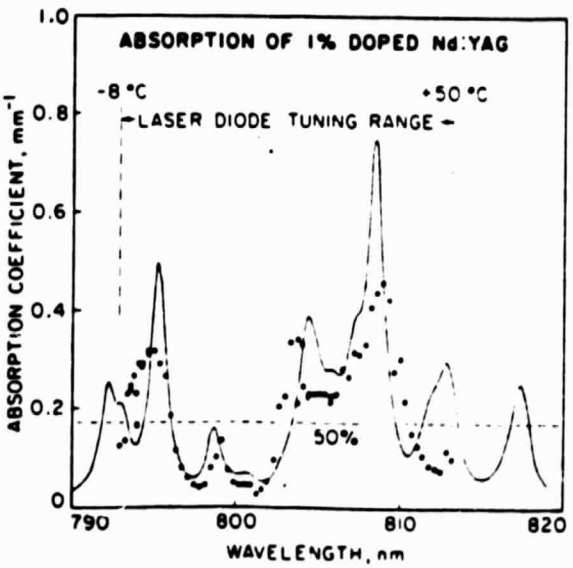

Fig. 3. Bulk absorptivity of Nd:YAG near 810 nm. Absorptivity α is defined by $I(x) = I(0)e^{-\alpha x}$, where $I(x)$ is the optical intensity at a position x. Data points are plotted as a function of diode temperature for a particular diode. The temperature range is indicated.

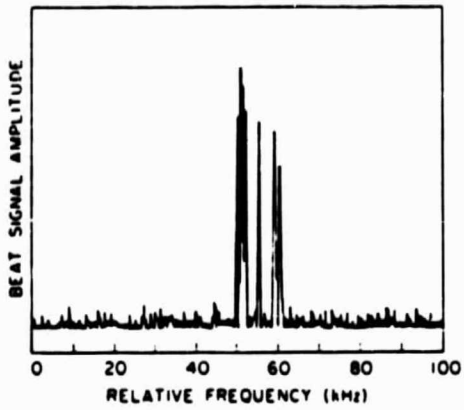

Fig. 4. Spectrum-analyzer trace of beating between independent lasers, recorded over 0.3 sec, shows a frequency jitter of 10 kHz.

There was also jitter of the beat signal, which was observed as random jumping of the signal between traces of the spectrum analyzer. The jitter was measured to be 10 kHz in 0.3 sec. Figure 4 is a spectrogram of the beat signal, recorded over a 0.3-sec period. During short intervals of about 5 msec when there was no jitter, we observed linewidths as low as 300 Hz, perhaps limited by the resolution of the spectrum analyzer.

The frequency drift was due to temperature drift. The jitter was due to relative motion between the laser-diode pump source and the Nd:YAG resonator, which resulted in the pump beam's wandering in the resonator mode volume and causing temperature fluctuations. A temperature-controlled and mechanically rigid mount is being built for further frequency stability studies.

Although we are now limited by frequency jitter of technical origin, it is of interest to find the ultimate frequency-stability limit of these lasers and to compare that limit with what is achievable with the diode laser itself. The fundamental limit to the frequency stability of the Nd:YAG oscillator is the Schawlow–Townes limit, which is given by[10]

$$\Delta\nu_{\text{laser}} = h\nu/2\pi t_c^2 P_0, \qquad (1)$$

where $h\nu$ is the laser photon energy and P_0 is the output power of the laser. The cold-cavity resonator decay time t_c is equal to $2nl/\delta c$, where n is the index of refraction of the material, l is the length of the laser resonator, c is the speed of light, and δ is the round-trip loss of the resonator, including output coupling. For a monolithic Nd:YAG laser the loss δ is 1% and the length l is 5 mm, whereas for a typical laser diode the loss is greater than 50% and the length is 0.3 mm. Although the other factors in Eq. (1) vary by small factors, the ratio l/δ is nearly 3 orders of magnitude larger for the monolithic Nd:YAG oscillators, as compared with a laser-diode oscillator. Thus the Schawlow–Townes limit is 6 orders of magnitude smaller. In addition, the semiconductor diode laser cannot reach the Schawlow–Townes limit because of an excess linewidth factor that may increase the linewidth by a factor of 30.[11] Laser diodes are unlikely to achieve linewidths of less than 1 MHz unless an external resonator is used, whereas our monolithic Nd:YAG laser at 1-mW output has a theoretical linewidth limit of less than 1 Hz.

The single-axial-mode power from a monolithic rod laser is limited by spatial hole burning. For the 5-mm rod, the threshold of the second axial mode occurs at 1.2 mW of output power. For the 3-mm rod it is 8 mW of output power. The threshold of the second axial mode can be accurately predicted by the theory of Danielmeyer.[12] This theory shows that the single-mode power limit is determined by a number of things but most signif antly by cavity length. Shorter cavities offer higher single-mode power. However, since laser-diode absorption is reduced with length, efficiency decreases. The high absorption of stoichiometric neodymium materials[7] may make possible high single-mode power from a laser-diode-pumped neodymium laser, but at the cost of amplifiability. An alternative approach is to use the recently demonstrated monolithic Nd:YAG ring-laser design (MISER).[13]

Active stabilization of the monolithic Nd:YAG oscillator may be achieved by the control of temperature, pressure, or electric field through the Kerr effect. Applications for the oscillator include metrology, fiber-optic sensing, and very-high-resolution spectroscopy. We expect an oscillator–amplifier combination to provide Fourier-transform-limited output in the multikilowatt range, with pulse lengths ranging from 1 μsec to 1 msec.

We thank Spectra Diode Laboratories Inc. and RCA Corporation for loans of diode lasers. This research was supported by NASA under grant NAG1-182. George J. Dixon is supported by a fellowship from the Office of Naval Research.

* Bingkun Zhou is a professor with the Department of Radio Electronics, Tsinghua University, Beijing, China. He was a visiting scholar at Stanford University during 1983–1984.

References

1. T. J. Kane, B. Zhou, and R. L. Byer, Appl. Opt. **23**, 2477 (1984).
2. Y. L. Sun and R. L. Byer, Opt. Lett. **7**, 408, (1982).
3. Specifications for RCA C86030E cw injection laser. RCA Corporation, New Holland Avenue, Lancaster, Pennsylvania 17604.
4. Spectra Diode Laboratories, Inc., 3333 North First Street, San Jose, California 95134.
5. J. Stone and C. A. Burrus, Fiber Integ. Opt. **2**, 19 (1979).
6. K. Washio, K. Iwamoto, K. Inoue, I. Hino, S. Matsumoto, and F. Saito, Appl. Phys. Lett. **29**, 720 (1976).
7. K. Kubodera and K. Otsuka, Appl. Opt. **18**, 3882 (1979).
8. D. Botez, Appl. Phys. Lett. **36**, 190 (1980).
9. *Selfoc Handbook*, NSG America, Inc., 136 Central Avenue, Clark, New Jersey 07066.
10. A. Yariv, *Quantum Electronics*, 2nd ed. (Wiley, New York, 1975).
11. C. H. Henry, IEEE J. Quantum Electron. **QE-18**, 259 (1982).
12. H. G. Danielmeyer, "Progress in Nd:YAG lasers," in *Lasers*, Vol. 4, A. K. Levine and A. J. DeMaria, eds. (Marcel Dekker, New York, 1976).
13. T. J. Kane and R. L. Byer, Opt. Lett. (to be published).

FEBRUARY 1985

VOLUME 10 NUMBER 2

Optics Letters

A publication of the

OPTICAL SOCIETY OF AMERICA

Monolithic, unidirectional single-mode Nd:YAG ring laser

Thomas J. Kane and Robert L. Byer

Ginzton Laboratory, Stanford University, Stanford, California 94305

Received October 1, 1984; accepted November 26, 1984

We have built a nonplanar ring oscillator with the resonator contained entirely within a Nd:YAG crystal. When the oscillator was placed in a magnetic field, unidirectional oscillation was obtained with a pump-limited, single-axial-mode output of 163 mW.

In this Letter, we describe a new solid-state laser design that achieves high single-mode output power by using a unidirectional nonplanar resonator. Excellent frequency stability is achieved because the ring resonator is constructed from a single Nd:YAG crystal. We refer to the design as a MISER (Monolithic Isolated Single-mode End-pumped Ring) design. We developed this source as an oscillator for a long-range coherent Doppler anemometer.[1] Other applications areas include coherent communications, coherent optical radar, and inertial rotation sensing.

Ideally, a continuous-wave homogeneously broadened laser should oscillate in a single axial mode. The laser transitions in Nd:YAG are primarily phonon broadened, so the assumption of homogeneity is met. However, when a Nd:YAG laser is contructed with a standing-wave linear resonator, the threshold of the second axial mode is near that of the first. At the nulls of the standing wave created by the initial axial mode, stimulated emission does not take place, and the gain is not saturated. This spatially modulated gain, termed spatial hole burning, allows other axial modes to reach threshold and oscillate.[2]

A unidirectional ring resonator has no standing wave, and therefore spatial hole burning is eliminated. Much higher single-mode power is available from a ring than from a linear resonator even without the addition of selective loss elements, such as étalons. Successful high-power, single-mode operation of unidirectional rings has been achieved with arc-lamp-pumped Nd:YAG oscillators[3] and with commercial dye lasers.[4]

Excellent frequency stability is possible when the resonator of a Nd:YAG laser is monolithic, that is, when it consists of reflective coatings applied directly to the surfaces of the Nd:YAG. Even better stability is possible when the pump source of the laser is a laser diode with stable output power. We recently reported a laser-diode-pumped Nd:YAG rod laser that has a frequency jitter in 0.3 sec of less than 10 kHz.[5] Because of spatial hole burning, output power in a single axial mode has been limited to 8 mW.

The objective of this work is to combine the advantages of ring lasers and monolithic lasers by constructing a unidirectional resonator entirely internal to a single crystal of Nd:YAG. The conventional way to design a unidirectional laser is to include a polarizer, a Faraday rotator, and a nonmagnetic polarization rotator, such as a half-wave plate in the resonator. All three of these functions, which together form an optical diode,[6] are incorporated into the MISER resonator design. As is shown in Fig. 1, the resonator is a single block of Nd:YAG incorporating four reflecting surfaces, which act as mirrors. The front face is convex to provide resonator stability and is coated to be a partially transmitting output coupler. The other three faces are flat and totally internally reflecting.

Most ring lasers use a resonator that is entirely within a plane. There are sometimes advantages to a nonplanar geometry that are worth the greater complexity. Dorschne at Raytheon has described a nonplanar helium–neon ring laser that, when used as a gyroscope, overcomes the problem of self-locking or lock-in.[7] Researchers in the Soviet Union have built nonplanar Nd:YAG ring lasers and have studied the mode structure, temporal dynamics, and polarization of these lasers.[8] Biraben[9] suggested that single-mode dye lasers

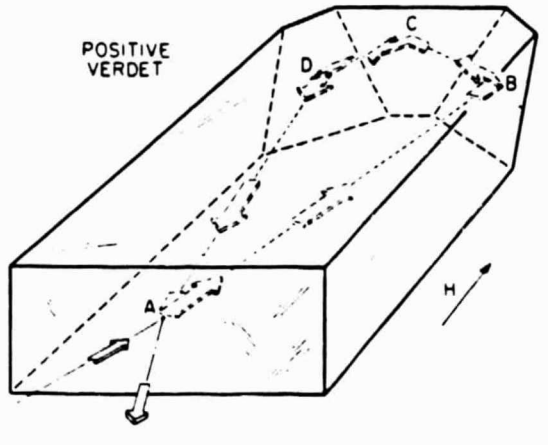

Fig. 1. The MISER laser design. Polarization selection takes place at the curved, partially transmitting face (point A). At points B, C, and D, total internal reflection occurs. A magnetic field H is applied to establish unidirectional oscillation. Magnetic rotation takes place along segments AB and DA. The focused pump laser beam enters the crystal at point A, and the output beam emerges at the same point.

0146-9592/85/020065-03$2.00

be constructed with a nonplanar ring-resonator geometry, for reasons similar to ours with the laser described here.

The nonplanarity of the MISER laser creates an effect that is analogous to rotation by a half-wave plate. The planes of incidence of the corner faces B and D are at an angle R to the plane of incidence of the front face. The plane of incidence of the top face is almost perpendicular to those of the corner faces. The rotation of the planes of incidence results in a net polarization (and image) rotation of $2R$ for a full round trip in the resonator.

The MISER design uses the Nd:YAG itself as a Faraday rotator. When there is a magnetic field applied along the long dimension of the Nd:YAG block, Faraday rotation takes place along the resonator segments AB (from the front face to the first corner) and DA (from the second corner back to the front face.) For one of the two traversal directions of the ring, the Faraday rotation subtracts from the polarization rotation that is due to the nonplanar design, whereas for the other direction, rotation is increased.

Nonnormal incidence on the output coupler face serves as the polarizer in this resonator. The P polarization is more strongly transmitted at the output coupler face, as the angle of incidence is not normal. The presence of this linear polarizer in the resonator favors the oscillation of polarization modes that are close to the S polarization. The oscillation cannot be in the linear S polarization, because in general any net rotation of polarization makes a linearly polarized mode impossible. The MISER would oscillate in a circular polarization if not for the birefringence that is due to the total internal reflection at points A, B, and C. This birefringence forces an elliptical polarization. If net rotation is reduced, then a polarization nearer pure S polarization becomes possible, and output coupling is reduced. When a magnetic field is applied, Faraday rotation cancels some of the geometrical rotation for one of the traversal directions, and the ring oscillates in that direction. A change in the sign of the magnetic field reverses the oscillation direction.

We have used Jones-matrix calculus to find numerically the eigenpolarizations and the difference in output coupling for the two directions of traversal. Our calculations show that when the magnetic rotation is small, maximum differential coupling occurs for an out-of-plane angle R of about 20°. At this angle the polarization is elliptical, with 89% of the power in the S polarization.

We have designed and constructed a MISER laser using Nd:YAG. The dimensions of the finished block were 38 mm × 13 mm × 3 mm. The angle of incidence at the output coupler was 7.8°, and the angle R between the output coupler plane of incidence and the corner face plane of incidence was 20°. All angles were specified with a tolerance of 0.08° (5 min). The output coupler was coated to be 99.2% reflecting in the S polarization and 98.8% reflecting in the P polarization at the angle of incidence used. The curvature of the output coupler face was 110 mm. For single-mode operation the crystal was placed in the field of a permanent magnet of 0.27-T average field. We measured the Verdet coefficient of Nd:YAG to be 103°/T m (Ref. 10), so the magnetic rotation in the segment AB is 1.1°. The differential loss between the two directions of traversal was calculated to be 0.01%.

The MISER laser was end pumped using an argon-ion laser (operating at 514.5 nm) focused with a 10-cm lens. The MISER threshold was reached at 0.15 W of pump power, and the slope efficiency was 5%. The transverse mode could always be limited to TEM_{00} by correctly aligning the pump laser and the ring resonator.

A Fabry–Perot étalon of free spectral range 1 cm^{-1} was used to observe the axial-mode structure. With a magnetic field present, oscillation was unidirectional, single mode, and stable. An interferogram of the single-mode output is shown in Fig. 2(a). Without a magnetic field, oscillation was bidirectional, multimode, and extremely noisy. Figure 2(b) is an inteferogram of the laser output without the magnetic field present.

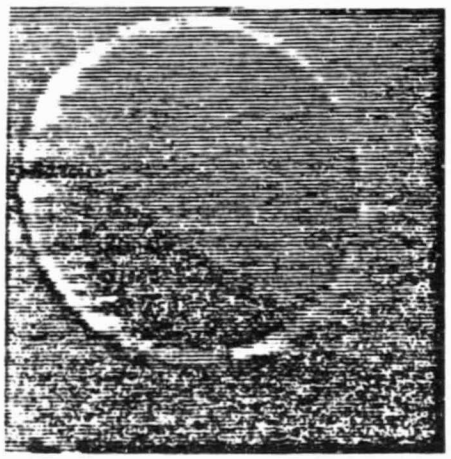

(a)

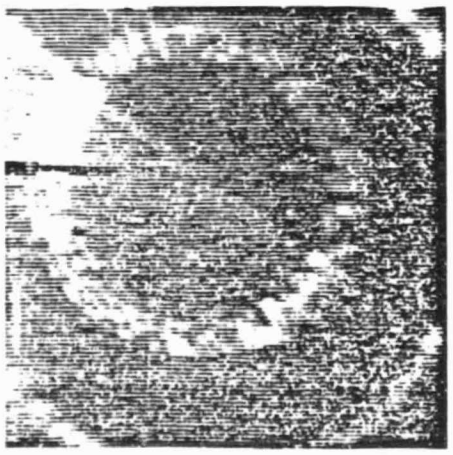

(b)

Fig. 2. (a) An interferogram of the MISER output with the magnetic field present, showing a single axial mode. (b) With the field removed, oscillation occurs in five axial modes. The free spectral range of the interferometer is 1 cm^{-1}; mode spacing is 0.064 cm^{-1}.

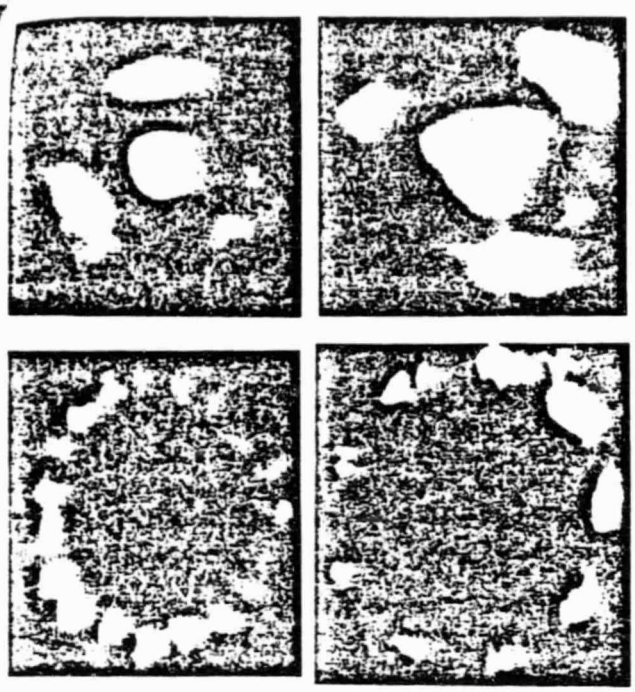

Fig. 3. The image rotation of a nonplanar resonator creates nonrectangular transverse-mode patterns. Four are pictured here.

With a field present, the MISER oscillated cw in a single direction and in a single mode up to an output power of 109 mW, which occurred at a 2-W pump power. At that level of pumping, bidirectional and multimode operation began. The output beam appeared to be badly distorted, indicating substantial thermal birefringence within the crystal. When a chopper was used to reduce the pumping duty cycle to 50%, single-direction, single-mode output was maintained up to the pump power limit of 3.1 W. Output at 1064 nm was 163 mW.

We also constructed and achieved unidirectional oscillation in a MISER using neodymium-doped gadolinium gallium garnet (Nd:GGG). Its dimensions were identical to those of the Nd:YAG MISER. The substantially greater Verdet constant of Nd:GGG (Ref. 10) is an advantage for this material. Detailed measurements were not made.

We made a beat-frequency measurement of the frequency stability of the argon-pumped MISER laser relative to a monolithic-rod Nd:YAG laser.[5] Jitter of 3 MHz in 1 sec was observed. Smaller MISER designs, when pumped with a semiconductor diode laser, should provide substantially better frequency stability.

When the pump beam is misaligned, higher-order transverse modes appear. The image rotation of the ring resonator breaks the rectangular symmetry of conventional resonators and leads to some unfamiliar transverse-mode patterns. Figure 3 contains photographs of some of the modes observed.

High scatter loss and low output coupling severely limit the efficiency of the MISER laser that we have tested. A 1/3-scale or smaller MISER design that uses low-doped, low-scatter Nd:YAG should improve efficiency and reduce threshold to the point that semiconductor laser-diode pumping would be possible. We believe that the present 109-mW limit on cw single-mode output is caused by thermal birefringence. Since any thermal effect is proportional to pump power, greater efficiency should lead to proportionally higher cw single-mode output power.

A laser-diode-pumped MISER laser could be a compact, efficient, and rugged high-power single-axial-mode oscillator. Applications include coherent communication through free space or through fibers using the 1321-nm transition of Nd:YAG. There may be remote-fiber-sensing applications for which the power available from a single-mode helium–neon laser is insufficient. If extreme frequency stability is achieved, then a MISER laser could be used as a compact and rugged ring-laser gyroscope. Stabilization may be possible by electrically tuning the magnetic field. There is a round-trip phase change that depends on polariztion rotation, and we have calculated that in Nd:YAG this will lead to a magnetic tuning coefficient of 20 MHz/T. Since a unidirectional ring laser is naturally isolated from light scattered back into the resonator from external optics, excellent frequency stability may be possible.

We thank Joe Vrhel, who fabricated the two MISER lasers, both of which oscillated on the first attempt. This research was supported by NASA under grant NAG1-182.

References

1. T. J. Kane, B. Zhou, and R. L. Byer, Appl. Opt. **23**, 2477 (1984).
2. H. G. Danielmeyer, in *Lasers*, Vol. 1, A. K. Levine and A. J. DeMaria, eds. (Marcel Dekker, New York, 1976).
3. A. R. Clobes and M. J. Brienza, Appl. Phys. Lett. **21**, 265 (1972).
4. Product literature for Spectra-Physics 380 series ring dye lasers and Coherent 699 series ring dye lasers.
5. B. Zhou, T. J. Kane, and R. L. Byer, in *Digest of the Thirteenth International Quantum Electronics Conference* (Optical Society of America, Washington, D.C., 1984), paper MEE2; B. Zhou, T. J. Kane, G. J. Dixon, and R. L. Byer, Opt. Lett. **10**, 62 (1985).
6. T. F. Johnson and W. Proffitt, IEEE J. Quantum Electron. **QE-16**, 483 (1980).
7. T. A. Dorschner, Proc. Soc. Photo-Opt. Instrum. Eng. **412**, 192 (1983).
8. Yu. D. Golyaev, K. N. Evtyukhov, L. N. Kaptsov, and S. P. Smyshlyaev, Sov. J. Quantum Electron. **11**, 1421 (1981), and references therein.
9. F. Biraben, Opt. Commun. **29**, 353 (1979).
10. Verdet constants were measured by comparison to the known value for the terbium-doped glass FR-5. For Nd:YAG, the constant was measured to be 103 ± 15°/T m. For GGG doped with 0.5% neodymium, we measured 387 ± 30°/T m.

Coherent LIDAR Anemometry Using Nd:YAG Lasers: System Design and Performance

Thomas J. Kane

Robert L. Byer

Ginzton Laboratory

Stanford University

Stanford, CA 94305, USA

ABSTRACT: We have designed and are now completing the construction of a coherent LIDAR anemometer using Nd:YAG lasers. The system and its components are described. Performance measurements to be made this spring will be described.

Coherent LIDAR Anemometry Using Nd:YAG Lasers: System Design and Performance

Thomas J. Kane
Robert L. Byer

Ginzton Laboratory
Stanford University
Stanford, CA 94305, USA

The coherent LIDAR system now under construction at Stanford is shown schematically in the figure. The nine components are described below.

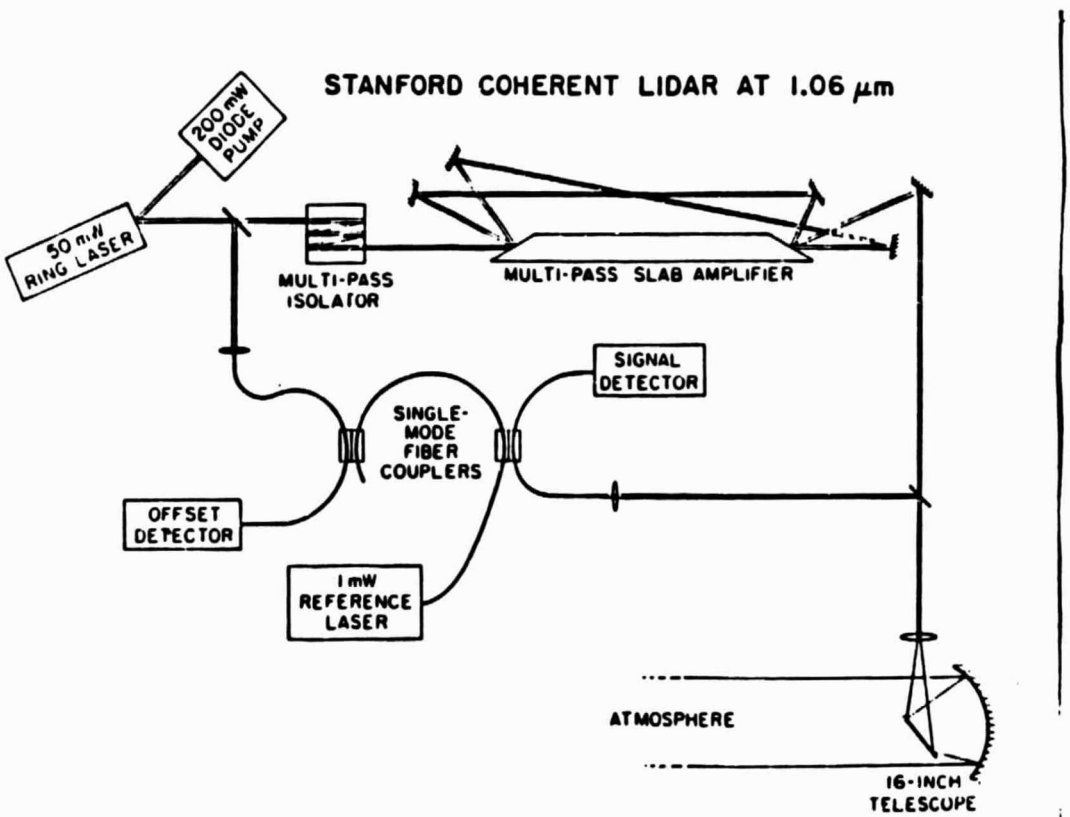

Figure 1. The coherent LIDAR anemometer is shown schematically.

1. 200 mW diode pump. A multiple-stripe phase-locked diode array provides the power to the Nd:YAG master oscillator.

2. 50 mW ring laser. An Nd:YAG laser of the monolithic ring design[1] is the master oscillator. It is designed for high single-mode power and good stability.

3. Faraday isolator. The output from the master oscillator passes through a permanent-magnet Faraday isolator. This reduces feedback into the master oscillator from the amplifier.

4. Multi-pass slab amplifier. The beam makes 3 passes through a flashlamp-pumped slab Nd:YAG amplifier. Gain in the amplifier has been measured at 20 decibels per pass. Thus the three passes will provide 60 decibels of gain. Not shown are spatial and temporal filters which provide isolation between stages of amplification and limit the duration of the transmitted pulse to 3 microseconds.

5. 16-inch telescope. The amplified beam is transmitted into the atmosphere by a telescope. The same telescope will collect the return signal from the atmosphere. Not shown are polarization optics which separate the transmitted and returned beams.

6. Single mode fiber couplers. The return signal is coupled into a single mode fiber. The single mode fiber provides a convenient and reliable way to ensure that only a single mode is detected, thus avoiding the excess noise of multi-mode detection. The single mode fiber couplers allow the various signals which must be heterodyned to be mixed together in a way that achieves essentially perfect spatial overlap.

7. 1 mW reference laser. The reference laser is designed for extreme stability at low power. We have demonstrated diode-pumped miniature Nd:YAG lasers with 10 kilohertz frequency jitter over a 0.3 second period[2].

8. Signal detector. Shot-noise limited heterodyne detection of the return

signal is accomplished with better than 50% efficiency using a quaternary photodiode.

9. Offset detector. The frequency difference between the reference and master oscillators is measured and controlled using the signal from the offset detector.

At this writing, most of the components are near completion, and system integration will begin soon. We will measure system output power, collection efficiency, signal-to-noise, and internally-generated frequency error. Results of these measurements will be presented.

References

1. T. J. Kane and R. L. Byer, "Monolithic, single-mode Nd:YAG ring laser," Optics Letters 10, p. 65, (1985).

2. B. Zhou, T. J. Kane, G. J. Dixon and R. L. Byer, "Efficient, frequency-stable laser-diode-pumped Nd:YAG laser," Optics Letters 10, p. 62, (1985).

High-gain Multi-pass Amplification in a Single Nd:YAG Slab

Thomas J. Kane

William J. Kozlovsky

Robert L. Byer

Ginzton Laboratory

Stanford University

Stanford, CA 94305

ABSTRACT: The zigzag slab geometry provides efficient high-gain unsaturated amplification, since many beams can be overlapped inside the slab and separated externally. We measured 23 dB single-pass gain, and are building a single-laser-head system with 60 dB net gain.

High-gain Multi-pass Amplification in a Single Nd:YAG Slab

Thomas J. Kane

William J. Kozlovsky

Robert L. Byer

Ginzton Laboratory

Stanford University

Stanford, CA 94305

We are building a coherent Doppler LIDAR system using Nd:YAG lasers. We are using a Master-Oscillator-Power Amplifier (MOPA) design, and thus need an amplifier with in excess of 60 dB gain. The zigzag slab provides a convenient way to efficiently build a high-gain multi-stage amplifier without building, pumping and cooling a number of laser heads, since the internal-reflection geometry allows many passes to be made through the same small volume.

Very high gain amplification of laser radiation is routinely accomplished by means of the "amplifier chain." In such a chain a number of gain regions exist, each pumped usually to the amplified spontaneous emission (ASE) limit. Some means of isolation between stages keeps the overall system from being overcome by ASE.

When the input pulse does not have adequate energy fluence to saturate the gain medium, then the first several stages of an amplifier chain may be inefficient, both in terms of energy, and usually more importantly, in terms of the cost of the hardware. It would be desirable to traverse a single stage several times.

The problem with multi-passing is beam separation. The active medium can be made large to allow for access from many angles, but this both increases the pump energy required and reduces the ASE-limited gain, which is highest for a long, narrow active volume. Polarization separation is possible for two or four passes, but is not always convenient.

A simple way to achieve high multi-pass gain is by taking advantage of the many paths that are possible through a zigzag slab. If the external angle of the beam passing through such a slab is varied in the plane of the zigzag, then the number of internal reflections will change, but the beam will continue to be confined to the slab until critical angle is reached. Figure 1 shows two possible paths through a short zigzag slab.

We have constructed a zigzag slab laser head which allows 5 possible paths, with 15, 17, 19, 21 and 23 internal reflections. The cross-section of the slab is 4 mm X 4 mm and the length 100 mm. We have measured the ASE-limited gain of the 23-bounce path to be 23 dB. This is higher than is generally achieved with a rod because the path length through the zigzag slab is longer than that through a rod of similar dimensions. The internal ray path is increased for a nearly-critical ray over a non-reflected ray by a factor of the index of refraction ratio at the reflecting interface. For Nd:YAG

cooled by water, this factor is 1.82/1.33 = 1.37. An unreflected ray in our slab would have a gain of 17 dB, or 50X.

We are building a set of spatial filters and mirrors to provide inter-stage isolation and re-injection of the amplified beam. Four stages of amplification will be provided, with spatial filters between each stage and acousto-optic time-gating between the second and third. We will report on the net gain, frequency chirp, noise figure and efficiency of this system, as well as the problem of beam deflection and distortion at high repetition rate. Since the zigzag slab design compensates for many of the thermal problems, operation at high repetition rate is expected to be possible.

We will use this amplifier as the power amplifier in a coherent LIDAR system. Other applications may be in the amplification of picosecond pulses, or in the amplication of the output of tuned, single-mode Nd:YAG oscillators, for spectroscopy or non-linear conversion.

Figure 1. A ray making 5 internal reflection in a zigzag slab overlaps a ray making 3 reflections, but the rays separate outside the slab.

5-BOUNCE
3-BOUNCE